ACCOUNTS
of chemical research

Roaming Atoms and Radicals: A New Mechanism in Molecular Dissociation

ARTHUR G. SUITS

Department of Chemistry, Wayne State University, Detroit, Michigan 48202

RECEIVED ON MARCH 4, 2008

CONSPECTUS

The detailed description of chemical reaction rates is embodied in transition state theory (TST), now recognized as one of the great achievements of theoretical chemistry. TST employs a series of simplifying assumptions about the dynamical behavior of molecules to predict reaction rates based on a solid foundation of quantum theory and statistical mechanics.

The study of unimolecular decomposition has long served as a test bed for the various assumptions of TST, foremost among which is the very notion that reactions proceed via a single well-defined transition state. Recent high-resolution ion imaging studies of formaldehyde unimolecular decomposition, in combination with quasiclassical trajectory calculations from Bowman and coworkers, have shown compelling evidence, however, for a novel pathway in unimolecular decomposition that does not proceed via the conventional transition state geometry. This "roaming" mechanism involves near dissociation to radical products followed by intramolecular abstraction to give, instead, closed shell products. This phenomenon is significant for a number of reasons: it resists easy accommodation with TST, it gives rise to a distinct, highly internally excited product state distribution, and it is likely to be a common phenomenon.

These imaging studies have provided detailed insight into both the roaming dynamics and their energy-dependent branching. The dynamics are dominated by the highly exoergic long-range abstraction of H from HCO by the "roaming" hydrogen atom. The energy-dependent branching may be understood by considering the roaming behavior as being descended from the radical dissociation; that is, it grows with excess energy relative to the conventional molecular dissociation because of the larger A-factor for the radical dissociation. Recent work from several groups has identified analogous behavior in other systems. This Account explores the roaming behavior identified in imaging studies of formaldehyde and considers its implications in light of recent results for other systems.

1. Introduction and Background

The study of unimolecular decomposition, by which we mean dissociation of isolated, energized molecules on the ground electronic state, provides an important foundation for understanding macroscopic chemical behavior.[1] This is so because virtually all of chemistry takes place as the result of decomposition of energized intermediates, formed either through collision (e.g., simple heating) or through chemical interaction. It is then given to transition state theory (TST) to make the connection between the microscopic, quantum behavior of isolated molecules and the macroscopic rates of chemical reactions.[2] This is achieved using a series of simplifying assumptions about the dynamical behavior of molecules and then by assembling it all on a solid footing of statistical mechanics.

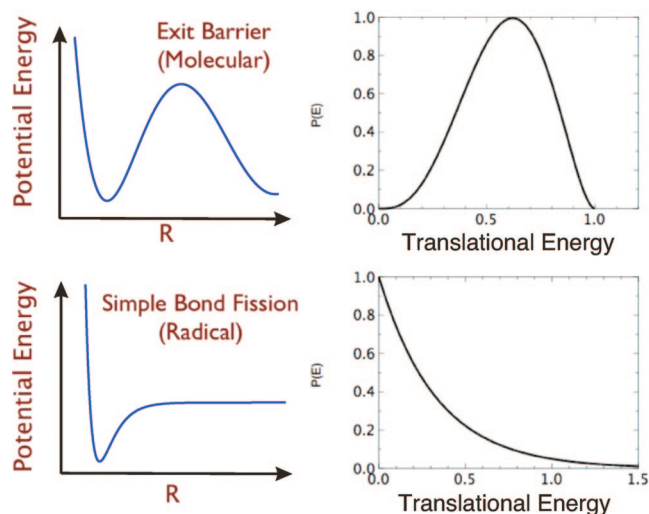Despite its simplifying assumptions, only rarely have real challenges to the validity of TST

FIGURE 1. Schematic potential energy profiles (left) and associated translational energy distributions (right) for two limiting dissociation cases.

appeared, and it is justifiably considered one of the great successes of theoretical chemistry. In this Account, we summarize the results of recent high-resolution ion imaging studies that, combined with sophisticated trajectory calculations from Bowman and co-workers, revealed a new "roaming" mechanism of unimolecular decomposition.[3−8] Furthermore, this roaming phenomenon resists easy accommodation within TST and may have broad practical consequences because it can cause product branching and product state distributions to differ significantly from TST predictions.

For molecular dissociation on the ground state, we may distinguish two distinct modes of decomposition, associated with different gross features of the potential energy surface (see Figure 1). The first, characteristic of closed shell molecules dissociating to closed shell products, features an exit barrier on the potential surface arising from electronic rearrangement that must accompany the breaking of the old bonds and formation of new bonds. The second, associated with simple bond fission to form open shell products, generally features no exit barrier. Each of these typically give characteristic translational energy distributions also shown in Figure 1: For dissociation over a barrier, much of the energy of the barrier appears in translational energy of the products, and the distribution peaks far from zero kinetic energy. This may be viewed as a result of Pauli repulsion between the closed shell product molecules newly formed in close proximity. For simple bond fission to radical products, however, the translational energy distributions peak at low energy, with most of the excess energy confined to internal degrees of freedom of the products.

For dissociation over a barrier, we naturally associate the transition state (TS) with the geometry at the top of the barrier. We define the reaction coordinate as those collective motions of the complex that lead from reactants to products and define a dividing surface at the TS "perpendicular" to the reaction coordinate in a multidimensional sense. Reaction is assumed to occur whenever the system passes through this dividing surface. TST then gives the rate of reaction roughly proportional to the number of accessible levels at the TS for a given energy. For reaction without a barrier, we can resort to an alternative definition of the TS by locating the dividing surface where the flux across it goes to a minimum. In this case variational methods may then be used to locate the TS at a given energy. These notions will be useful as we consider a third kind of dissociation, roaming, in the pages that follow.

The work described here represents a state-to-state investigation of formaldehyde photodissociation. Formaldehyde has proven to be a marvelous "laboratory" for the investigation of a range of issues in fundamental chemical physics, dating from very early spectroscopic studies[9] to more than a decade of detailed dynamics investigations from the Moore group at Berkeley.[10−21] Among the many reasons for the ongoing interest in formaldehyde are its relative simplicity and the fact that well-defined metastable excited-state levels may be prepared by convenient electronic excitation in the ultraviolet but dissociation occurs on the ground-state following internal conversion. Our entry into the study of this benchmark system was prompted by the existence of a newly developed, accurate global potential energy surface for the molecule,[22] as well as a remarkable paper by van Zee et al.[21] reporting some rather puzzling features of the dynamics. Armed with new experimental techniques, outlined in the next section, we believed we were in a position to look deeper into the questions raised by the van Zee work.

Schematic cuts through the relevant potential surfaces for formaldehyde[22] are presented in Figure 2. Both of the aforementioned surface types are present for ground-state dissociation: a high barrier to decomposition to closed shell products H_2 and CO and, at slightly higher energy, the barrierless radical dissociation giving H + HCO. At yet higher energy, radical dissociation on the triplet surface may occur over a small barrier. This raises a number of other interesting issues that have been examined in detail by Kable and others[23−27] but will not be considered further here. The molecular dissociation channel was the focus of Moore's efforts, and a key aspect of their work was interest in the TS geometry and the detailed dynamics of energy and angular momentum parti-
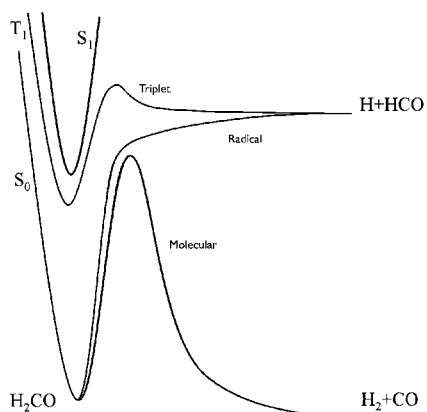
FIGURE 2. Schematic potential energy curves for formaldehyde dissociation.

tioning in the exit channel. They found that CO rotational distributions peaked at very high levels, as seen reproduced in Figure 3, and they ascribed this to the strong impulse (from the barrier) acting on the skewed, planar TS geometry. For dissociation at energies below the radical dissociation threshold, only this main, high j_{CO} peak is seen (e.g., the lowest distribution in Figure 3). Above the radical threshold, however, a new component appears: a small shoulder on the main peak extending to very low rotational levels. It is seen to varying degrees on most other distributions in Figure 3. This shoulder was the focus of the van Zee paper, and they ascribed it either to some influence of the radical channel or to anharmonicity of the TS at this energy giving rise to dissociation from distorted geometries.

We should note that some aspects of the roaming dynamics described here were anticipated in studies of the $O + CH_3$ reaction reported by Leone and co-workers[28] and examined theoretically by Harding and Klippenstein. CO was clearly identified as a signifiant product in the experiments, but no TS could be found. Direct dynamics calculations[29] subsequently revealed an "over-the-ridge" mechanism leading to H_2 formation, with the CO resulting from decomposition of hot HCO. A roaming-like mechanism was proposed earlier by Jackson and co-workers in the reaction $CN + O_2$ to account for formation of CO + NO products well below the four-center transition state.[30] Moreover, roaming may be viewed as one extreme example of reactions that occur far from the minimum energy path (MEP), and numerous examples have been found in which non-MEP dynamics give rise to distinct product state distributions.[31–34] This is discussed further in later sections.

2. Experimental Approach

These experiments were performed using the DC slice imaging technique,[35] a variant of the velocity map version[36] of the
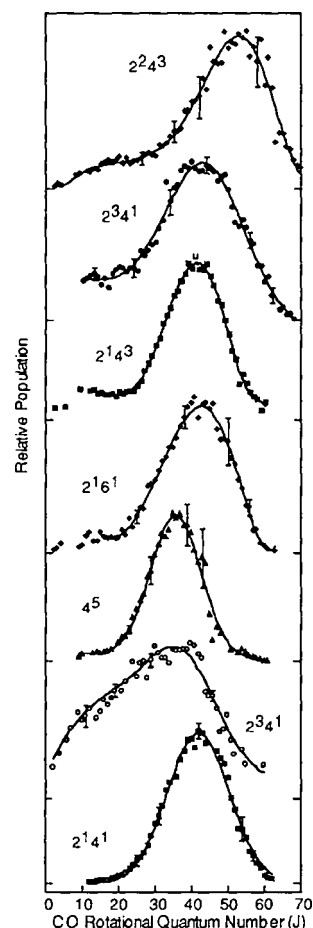

FIGURE 3. CO rotational distributions following dissociation of formaldehyde via the indicated transition. R. D. van Zee et al., J. Chem. Phys. 1993, 99, 1664. Copyright 1993, American Insititute of Physics. Reproduced by permission.

ion imaging technique.[37] A schematic of the experiment is shown in Figure 4. Formaldehyde gas seeded in argon is released from a pulsed nozzle into a vacuum chamber, then skimmed before entering the main interaction chamber. The resulting molecular beam is cooled rotationally to ~10 K. Formaldehyde molecules are then excited by a UV laser tuned to a single rotational transition into the first excited state. The molecules undergo internal conversion back to the ground state and dissociatiate some tens to hundreds of nanosconds later. Single rovibrational levels of the product CO molecules are then ionized using a second UV laser.

The product ions, expanding with the nascent velocity distribution of the original neutrals, are accelerated down a time-of-flight tube via a series of electrodes that achieve both velocity focusing and stretching of the ion cloud along the flight direction. At the end of the flight tube the ions strike a position-sensitive detector that is gated to detect only the portion of the ion cloud whose center-of-mass velocity is parallel to the detector plane, giving a "slice" of the recoiling
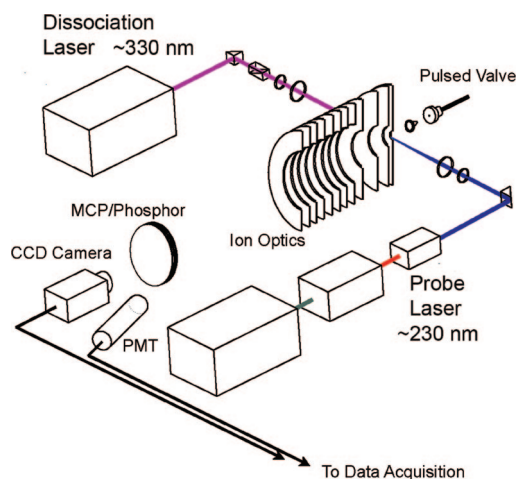
FIGURE 4. Schematic of DC sliced imaging experiment.

product distribution. The detector is viewed by a CCD camera, and the images are captured by a computer where they are processed and integrated.[38] The images directly yield the neutral velocity distribution in the center of mass frame: the distance from the center is simply proportional to the recoil speed, and this can readily be made quantitative with appropriate calibration. The total translational energy is then determined by invoking conservation of linear momentum between the CO and H_2 products.

In addition to ion imaging data, we also record photofragment excitation (PHOFEX) spectra. In this case, the detection laser is fixed on a single CO quantum state, and the excitation laser is scanned. These spectra then give the relative probability for a given formaldehyde transition to yield population in a particular CO product state.

3. Roaming Atoms

A series of CO images are shown in Figure 5 for the indicated rotational level of $v = 0$ following excitation of formaldehyde just ~30 cm^{-1} above the radical dissociation threshold.[3,4] (Moore and co-workers have shown the product CO is produced predominantly in $v = 0$.) Accompanying each image is the total translational energy distribution obtained by analysis of the image and transformation from CO velocity to total center-of-mass translational energy. Because the initial internal energy in H_2CO is negligible (by virtue of the inherent cooling of the supersonic molecular beam) and because the internal energy of the CO is determined by the quantum state that we detect, conservation of energy ensures that the internal energy in the undetected H_2 is also fixed for each point of the translational energy distribution. Structure in the translational energy distribution thus directly reflects structure in the H_2 internal energy distribution. The four rings in the image in

Figure 5A, associated with CO($v=0,j=45$), represent four vibrational levels, $v = 0-3$, in the product H_2; the outermost ring, that is, the greatest recoil energy, is thus $v = 0$ as indicated. The size of each peak tells us the yield of a given vibrational level of H_2 formed in conjunction with the detected quantum state of CO. We can also obtain the H_2 rotational distributions by fitting these vibrational peak profiles, but this is beyond the scope of our present discussion. In any case, the detailed information contained in Figure 5 was not available in the earlier experiments from the Moore group. We now have the full quantum state distribution for the undetected product H_2 formed in coincidence with a given quantum state of CO. This *correlated state information* gives deep new insight into the dynamics. A more detailed review of our correlated state investigations in formaldehyde, including the molecular channel, was recently published.[39] The interested reader is referred there for more information.

As we discussed in the introduction, the distribution in Figure 5A is expected: it peaks at high recoil energy as much of the energy of the exit barrier is released into recoil between the products. When we look at the images in Figure 5B,C, recorded on the lower rotational levels of CO (toward the shoulder seen in the van Zee data reproduced in Figure 3), we see something very different. For $j_{CO} = 28$, in addition to the outer rings corresponding to H_2, $v = 0-3$, we see a series of inner rings representing coincident formation of H_2 in very high vibrational levels, up to $v = 7$ and 8. This bimodal vibrational distribution is seen clearly in the translational energy distributions as well. Finally, we consider the $j_{CO} = 15$ image shown in Figure 5C. Now, only the slow component appears, indicating that only very high vibrational levels of H_2 are formed in coincidence with CO in this low rotational level.

This bimodal distribution clearly indicates two dynamically distinct pathways to dissociation. The first, giving low vibrational levels of H_2 in conjunction with high rotational levels of CO, is the expected result of dissociation over the barrier.[16,17] The second, giving high vibrational levels of H_2 with low rotational excitation of CO, is surprising and unlikely to result from dissociation over the barrier. To understand its origin, we turned to quasiclassical trajectory calculations from Bowman and co-workers performed on the new ab initio potential energy surface.[3,4] These calculations also gave a bimodal distribution in good agreement with experiment. Furthermore, the trajectories could be examined individually to gain deeper insight into their origin.

Several such trajectories are plotted in Figure 6.[40] In these trajectory visualizations, developed by F. Suits at IBM using trajectory data from Bowman and co-workers, only the H atom
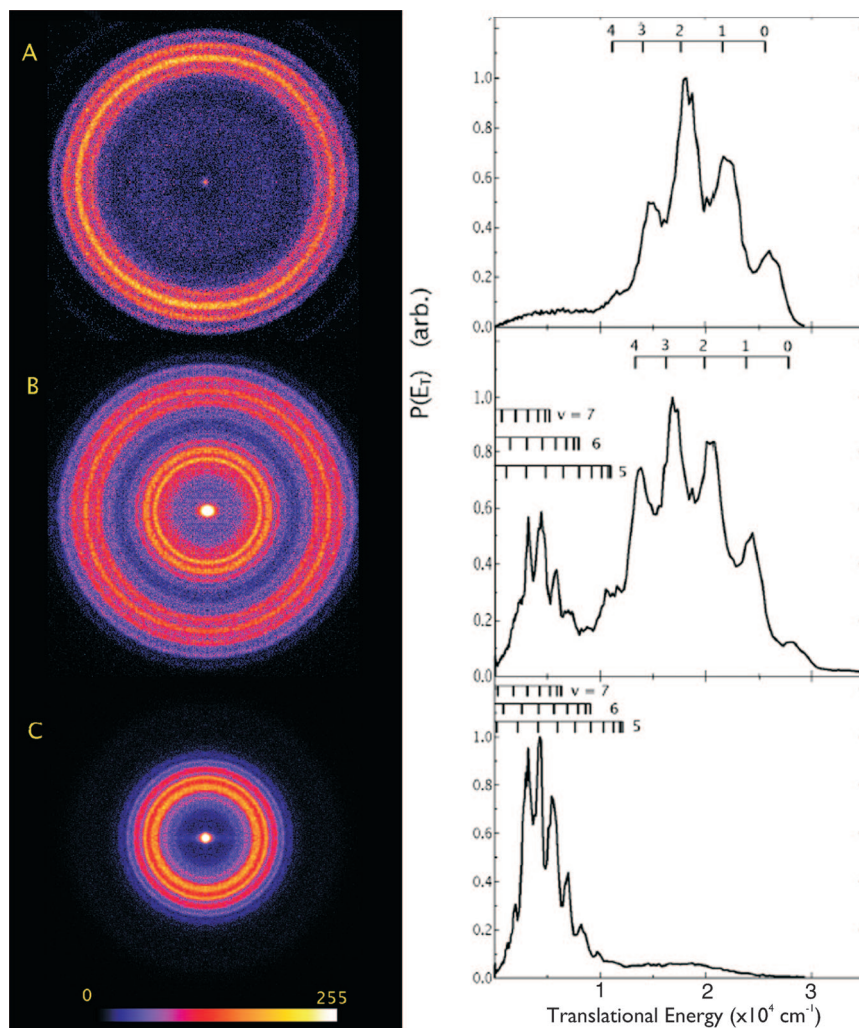
FIGURE 5. DC sliced images (left) of CO for dissociation of H_2CO on the $2^1 4^3$ band for (A) $j_{CO} = 40$, (B) $j_{CO} = 28$, and (C) $j_{CO} = 15$ and translational energy distributions (right) obtained from the corresponding images at left. Markers indicate correlated H_2 vibrational levels for $j_{H_2} = 5$ (for $v = 0-4$) or rovibrational levels (for $v = 5-7$).

motions are shown with the instantaneous speed encoded in color. Figure 6, top, shows a trajectory leading to CO ($v = 0$, $j = 41$) along with H_2 ($v = 1$, $j = 6$), that is, the conventional dissociation over the barrier. Complex motion is seen of the highly energized H_2CO until the transition state geometry is encountered, after which H_2 is promptly formed and emitted to the right of the figure. The plot in Figure 6, middle, corresponding to production of CO ($v = 0$, $j = 6$) along with H_2 ($v = 7$), is very different. The energy accumulates in one C−H bond until the H atom is nearly free, leaving HCO with very little internal energy. The H atom roams at large C−H distance (3−4 Å) where the potential is nearly flat. The HCO can be seen to rotate out of the plane containing the roaming atom. Finally, the roaming atom returns to abstract the remaining H atom, forming highly vibrationally excited H_2. This high vibrational excitation in H_2 is just as one would expect for the H + HCO abstraction: this highly exothermic, barrierless reaction

will occur at long range giving rise to highly excited H_2 and low recoil energy. Figure 6, bottom, shows another roaming trajectory for comparison.

The dynamics seen in Figure 6, middle and bottom, and reproduced in many other trajectories clearly account for the second pathway. When enough energy accumulates in one C−H bond to allow near-dissociation to radical products, roaming may occur ultimately leading to intramolecular H abstraction. This is significant for a number of reasons, both practical and academic, and these are discussed in detail in section 4.

4. Energy Dependence and Branching

We have seen that this novel roaming mechanism takes place at an energy just a few cm^{-1} above the threshold for the radical dissociation. Could it be strictly a threshold phenomenon?
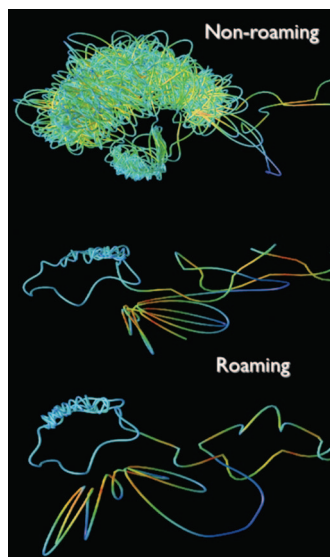
FIGURE 6. Plots of a sample trajectories. Only H atoms are shown. H atom speeds are encoded in trajectory color. Upper trajectory is a typical nonroaming event, while the lower two are characteristic roaming events.
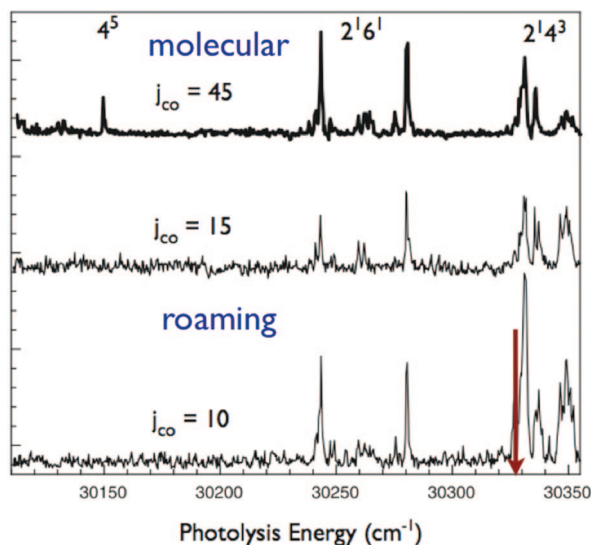

FIGURE 7. PHOFEX scan across the radical dissociation threshold (30329 cm^{-1}) for indicated CO rotational levels showing the occurrence of roaming below the radical threshold.

If not, what is its energy dependence? Can it occur below the radical dissociation threshold? To gain insight into these issues, we first employ PHOFEX spectroscopy. We have just established that low rotational levels of CO occur exclusively via the roaming mechanism, while high rotational levels of CO only result from the dissociation over the barrier. We thus use these as markers for the two respective pathways and examine their dependence as we scan the excitation laser.

PHOFEX results obtained below the radical threshold are shown in Figure 7. The structure in these spectra represent transtions between the ground state and first excited state in
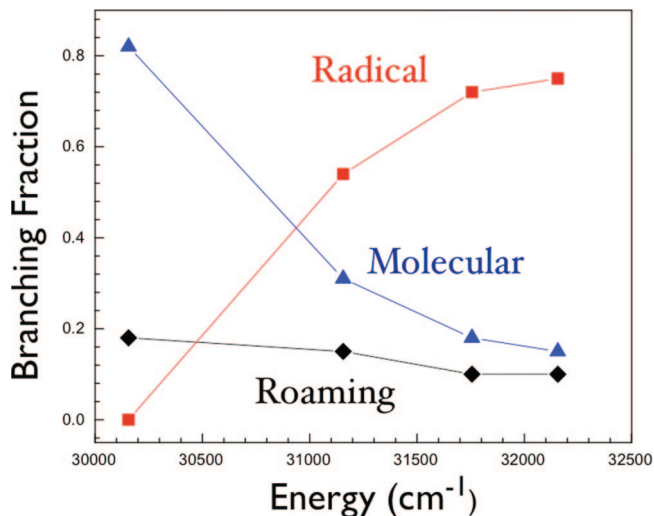

FIGURE 8. Energy-dependent multichannel branching.

formaldehyde. For the spectrum recorded on $j_{CO} = 45$ (top), all formaldehyde transitions in this vicinity are seen. This is expected for the conventional molecular channel, because the energy here is >300 cm^{-1} above the molecular dissociation barrier. For spectra obtained via the lower rotational levels, roaming dissociation is clearly seen 90 cm^{-1} below the radical threshold, as indicated by the persistence of the low j_{CO} signals there. However, at 150 cm^{-1} below, the roaming signal disappears (note the absence of the 4^5 transition in the two lower scans). The roaming mechanism threshold is thus somewhere between 90 and 150 cm^{-1} below the radical asymptote; the implications of this will be considered further in the next section. We have also confirmed, using imaging, that these probe transitions are indeed representative of the two distinct dissociation mechanisms.

We have thus established the lower energy limit for roaming, but what happens as we increase the energy? In a series of studies, we recorded both PHOFEX spectra and images up to 3000 cm^{-1} above the radical asymptote, even into the region above the triplet dissociation barrier.[5,40] Again, roaming was clearly seen in the images obtained on lower rotational levels. Furthermore, the PHOFEX spectra were scaled after detailed characterization of a single transition so that the relative yield of $j_{CO} = 15$ and 45 could be used to give the overall yield of the roaming pathway relative to the TS pathway. Then, by scaling these results relative to the radical yield using the QCT calculations, we obtained the overall multichannel branching shown in Figure 8. The results show that the roaming yield grows rapidly relative to the conventional molecular channel, and at the highest energies that we have studied, more than half of the molecular products are formed by roaming. However, the radical channel grows in importance very rapidly with energy, owing to the large A factor

(and loose transition state) for this pathway. The result overall is that the relative yield of the molecular channel drops with energy as the radical channel takes over, while the roaming yield overall is nearly flat or dropping slowly with increasing energy.

5. What Does It All Mean? Roaming Dynamics and Implications for Transition State Theory

We have seen that these two dynamical pathways are clearly different. If we look at the product state distribution or closely examine the trajectories, we see quite distinct populations. The trajectories show that the products that we associate with the conventional mechanism all follow very close to the minimum energy path and attain a configuration closely resembling the geometry of the TS saddle point. The roaming events, on the other hand, are clearly very different. They all appear to reach a C−H distance of 3−4 Å, and typically the roaming atom is found at times out of the plane of the HCO. This raises an intriguing question. We know that the radical dissociation itself is barrierless, but is there a distinct transition state for roaming? Recent calculations from Klippenstein and Harding[41] have identified just such a transition state, although its unusual qualitities led them to prefer to call it a transition state "region". Their TS geometry shows the roaming atom out of the HCO plane and at a distance of 3.4 Å. However, the frequencies that they calculate clearly correspond to an isolated HCO molecule and a nearly free H atom. The energy that they find for this TS is 40 cm^{-1} below the radical asymptote, not far from our observation of a cutoff of the roaming pathway somewhere between 90 and 150 cm^{-1} below the radical limit.

We can thus understand the energy-dependent trends in Figure 8 if we simply recognize roaming as derived from the radical dissociation, that is, it is a frustrated radical dissociation event. We then expect the energy dependence to parallel that of the radical channel. It has little to do with the conventional molecular dissociation and its associated tight transition state. Instead, as shown by the subthreshold behavior in Figure 7, we can see that there is a finite energy window, extending ~100 cm^{-1} below the H + HCO asymptote, for which roaming may occur. This is the region for which the system has enough energy to overcome the barrier but not enough to dissociate directly to radical products. This is the "roaming window". The radical asymptote here is one in which the product HCO has no internal energy, of course. However, we can imagine another asymptote leading to HCO in some

other rovibrational level. It is reasonable to imagine that this level may have an analogous TS 100 cm^{-1} below it as well. In other words, the location of the TS in this case may be simply offset by the HCO product energy level, because they are not likely to be coupled at this long range. Then, by assuming a similar roaming window ~100 cm^{-1} below each possible HCO product state, we find a continuum in which roaming may occur, from ~100 cm^{-1} below the radical threshold, up to the three-body dissociation level forming H + H + CO. As the energy increases, the larger A factor implies that branching to the radical dissociation will grow rapidly. However, the fraction of HCO levels supporting this roaming TS may not grow quite as rapidly. The roaming yield that we expect will be a roughly constant or perhaps a slowly falling fraction of the radical channel yield, just as seen in Figure 8.

Now we look more deeply at the implications of this. Does TST really fail in describing this phenomenon? Some might prefer to think of the real TS, at this fairly high energy over the molecular barrier, as spanning a broad swath of the molecular configuration space and note that it is imprecise to think of the configuration at the top of the barrier as the TS geometry *per se*. Instead, they might argue, if we trust in TST and bring all the power of the variational methods to bear, we would find, in some sense, these two TSTs that we have found are really one. This may be true, but it certainly has not been demonstrated. In any case, this perspective does not readily lead us to make practical predictions of branching or product state distributions or reaction rates. We may rescue the theory, only to find it useless for the problem. Instead, if we see roaming as related to the radical dissociation channel and describe it separately from the pathway over the barrier, we can achieve a succinct description of the problem and a deeper understanding of the dynamics. We find, in fact, at all energies studied, that the products that appear over the barrier pass very close to the minimum energy path. Only the roaming events stray very far from it. The barrier-path/radical dissociation dichotomy represents a useful "basis" in which to describe the problem, although a strict variational treatment may be equally valid. This discussion takes us back to the van Zee paper, in which two alternative accounts of the unusual dynamics in H$_2$CO were offered. One suggestion was that the dynamics imply some participation of the radical channel in the molecular decomposition. The second was that "anharmonicity at the TS" could lead to dissociation from geometries quite distinct from that at the top of the barrier. We can now see these two alternative descriptions as related to

the two "basis sets" we have just discussed, and they may represent two alternative descriptions of the same underlying dynamics.

This is a good opportunity to make a connection with other recent investigations of novel aspects of reaction dynamics. Hase and co-workers have shown that reactions deviating far from the minimum energy path (MEP) are not uncommon, and these often give rise to distinct, vibrationally excited product state distributions.[31–33] It is interesting to consider the roaming mechanism in this light. Roaming obviously represents a striking deviation from the MEP for the molecular dissociation, and the products are formed with a dramatically different product state distribution, so it clearly fits under the umbrella of non-MEP reactions. But perhaps roaming is even more distinctive than would be suggested by the non-MEP categorization alone. In fact, in a sense it does follow the minimum energy path, an alternative MEP through an alternative TS, ultimately to the same products. These issues clearly merit deeper theoretical investigation.

6. Outlook: Roaming Radicals

One question that we have not yet addressed is how general this phenomenon might be. Might we hope to see roaming atoms in other systems? And if atoms can roam to give surprising products or product state distributions, might radical fragments of molecules roam as well? Apparently both questions have been answered in the affirmative. In studies of acetaldehyde photodissociation[42] (which, we note, is formaldehyde with a methyl replacing one of the H atoms), Houston and Kable have seen evidence for roaming analogous to that in formaldehyde. They observed broad CO Doppler profiles for high rotational levels of CO, implying high recoil speeds as expected for the dissociation over the barrier. For the low rotational levels, the Doppler profiles were narrow, implying low recoil speeds just as we saw for CO from roaming in H_2CO. In the acetaldehyde case, however, it is clear from the energetics that methyl must be the roaming species, because the threshold for methyl loss is lower than that for H loss. These results have been duplicated in imaging experiments recently as well.[43] Houston and Kable also supported their arguments with vector correlation measurements. They were able to show that, for the fast CO products, the angular momentum vector was largely perpendicular to the recoil direction. This is the necessary outcome if the methyl center of mass, H atom, and CO are coplanar, as at the top of the barrier. For the roaming trajectories, as we have seen in H_2CO, deviation from planarity is expected, and the degree of align-

ment of the angular momentum vector with respect to the recoil direction may thus be lost. This issue of vector correlations in roaming reactions will be an interesting one to pursue. The results they found for the j_{CO} dependence of this correlation were entirely consistent with the roaming picture for the low j products. Moreover, theory has recently also provided support for a "roaming methyl" in acetaldehyde dissociation.[41,44] A "roaming TS region" has been identified, and it is quite analogous to that seen for formaldehyde. Recent calculations have shown that the roaming-type dynamics are likely even more significant than suggested by the experiments.[44]

We might next wonder just how general this is. Is there anything peculiar about these systems? Will this be found in elsewhere? It is not difficult now, based on what we have learned here, to draw some general conclusions. For roaming to occur, there must be a barrierless dissociation pathway that is not too far above other dissociation pathways so that it may be populated with some likelihood. Then, there must be a barrierless path for the relevant abstraction reaction, and it should be strongly exoergic. Neither of these conditions is unusual for closed shell molecules. The key issue for the future investigation of these phenomena is in fact more practical. Formaldehyde is an ideal case from several points of view. State-resolved CO detection by ionization is quite sensitive, and the large energy spacing of the H_2 cofragment means that it is easy to isolate the distinct components in the correlated state distributions. In the acetaldehyde case already, this is problematic. The distributions are not clearly bimodal, and theory will be required to unravel them fully. For other systems, this may become very challenging indeed. Roaming dynamics may be everywhere, but it will take sharp eyes, powerful techniques, and strong interplay between theory and experiment to see it.

BIOGRAPHICAL INFORMATION

Arthur G. Suits is Professor of Chemistry at Wayne State University. His group is engaged in studies of fundamental reaction dynamics, astrochemistry, chemical physics, and new experimental directions in ion imaging and mass spectrometry.

REFERENCES

1 Baer, T.; Hase, W. L. *Unimolecular Reaction Dynamics*; Oxford University Press: New York, 1996.

2 Steinfeld, J. I.; Francisco, J. S.; Hase, W. L. *Chemical Kinetics and Dynamics*, 2nd ed.; Prentice Hall: Upper Saddle River, NJ, 1999.

3 Townsend, D.; Lahankar, S. A.; Lee, S. K.; Chambreau, S. D.; Suits, A. G.; Zhang, X.; Rheinecker, J.; Harding, L. B.; Bowman, J. M. The Roaming Atom: Straying from the Reaction Path in Formaldehyde Decomposition. *Science* **2004**, *306*, 1158–1161.

4 Lahankar, S. A.; Chambreau, S. D.; Townsend, D.; Suits, F.; Farnum, J.; Zhang, X.; Bowman, J. M.; Suits, A. G. The Roaming Atom Pathway in Formaldehyde Decomposition. *J. Chem. Phys.* **2006**, *125*, 044303.

5 Lahankar, S. A.; Chambreau, S. D.; Zhang, X.; Bowman, J. M.; Suits, A. G. Energy Dependence of the Roaming Atom Pathway in Formaldehyde Decomposition. *J. Chem. Phys.* **2007**, *126*, 044314.

6 Zhang, X.; Rheinecker, J. L.; Bowman, J. M. Quasiclassical Trajectory Study of Formaldehyde Unimolecular Dissociation: H(2)CO-->H2 + CO, H + HCO. *J. Chem. Phys.* **2005**, *122*, 114313.

7 Rheinecker, J. L.; Zhang, X.; Bowman, J. M. Quasiclassical Trajectory Studies of the Dynamics of H2CO on a Global ab Initio-Based Potential Energy Surface. *Mol. Phys.* **2005**, *103*, 1067–1074.

8 Zhang, X.; Bowman, J. M. New Insights on Reaction Dynamics from Formaldehyde Photodissociation. *Phys. Chem. Chem. Phys.* **2006**, *8*, 321–332.

9 Dieke, G. H.; Kistiakowsky, G. B. The Rotational Structure of the Ultra-Violet Absorption Bands of Formaldehyde. *Proc. Natl. Acad. Sci. U.S.A.* **1932**, *18*, 367–372.

10 Yeung, E. S.; Moore, C. B. Photochemistry of Single Vibronic Levels of Formaldehyde. *J. Chem. Phys.* **1973**, *58*, 3988–3998.

11 Yeung, E. S.; Moore, C. B. Predissociation Model for Formaldehyde. *J. Chem. Phys.* **1974**, *60*, 2139–2147.

12 Houston, P. L.; Moore, C. B. Formaldehyde Photochemistry: Appearance Rate, Vibrational Relaxation, And Energy Distribution of the Carbon Monoxide Product. *J. Chem. Phys.* **1976**, *65*, 757–770.

13 Weisshaar, J. C.; Baronavski, A. P.; Cabello, A.; Moore, C. B. Collisionless Decay, Vibrational Relaxation, And Intermediate Case Quenching of S1 formaldehyde. *J. Chem. Phys.* **1978**, *69*, 4720–4731.

14 Ho, P.; Bamford, D. J.; Buss, R. J.; Lee, Y. T.; Moore, C. B. Photodissociation of Formaldehyde in a Molecular Beam. *J. Chem. Phys.* **1982**, *76*, 3630–3636.

15 Moore, C. B.; Weisshaar, J. C. Formaldehyde Photochemistry. *Annu. Rev. Phys. Chem.* **1983**, *34*, 525–555.

16 Bamford, D. J.; Filseth, S. V.; Foltz, M. F.; Hepburn, J. W.; Moore, C. B. Photofragmentation Dynamics of Formaldehyde: Carbon Monoxide(v,J) Distributions As a Function of Initial Rovibronic State and Isotopic Substitution. *J. Chem. Phys.* **1985**, *82*, 3032–3041.

17 Debarre, D.; Lefebvre, M.; Pealat, M.; Taran, J. P. E.; Bamford, D. J.; Moore, C. B. Photofragmentation Dynamics of Formaldehyde: Hydrogen (H2(v, J)) Distributions. *J. Chem. Phys.* **1985**, *83*, 4476–4487.

18 Moore, C. B.; Bamford, D. J. State-Selected Photodissociation Dynamics of Formaldehyde. *Laser Chem.* **1986**, *6*, 93–102.

19 Butenhoff, T. J.; Carleton, K. L.; Chuang, M. C.; Moore, C. B. Vector and Product Quantum-State Correlations for Photofragmentation of Formaldehyde. *J. Chem. Soc., Faraday Trans. 2* **1989**, *85*, 1155–1167.

20 Carleton, K. L.; Butenhoff, T. J.; Moore, C. B. Photodissociation Dynamics of Formaldehyde: Molecular Hydrogen (v, J) Vector Correlations. *J. Chem. Phys.* **1990**, *93*, 3907–3918.

21 van Zee, R. D.; Foltz, M. F.; Moore, C. B. Evidence for a Second Molecular Channel in the Fragmentation of Formaldehyde. *J. Chem. Phys.* **1993**, *99*, 1664–1673.

22 Zhang, X.; Zou, S.; Harding, L. B.; Bowman, J. M. A Global ab Initio Potential Energy Surface for Formaldehyde. *J. Phys. Chem. A* **2004**, *108*, 8980–8986.

23 Terentis, A. C.; Kable, S. H. Near Threshold Dynamics and Dissociation Energy of the Reaction H2CO->HCO+H. *Chem. Phys. Lett.* **1996**, *258*, 626–632.

24 Terentis, A. C.; Waugh, S. E.; Metha, G. F.; Kable, S. H. HCO (N,Ka,Kc,J) Distributions from near-Threshold Photolysis of H2CO (J,Ka,Kc). *J. Chem. Phys.* **1998**, *108*, 3187–3198.

25 Yin, H.-M.; Nauta, K.; Kable, S. H. Fully State-Resolved Photodissociation of Formaldehyde, H2CO -> H + HCO: K Conservation and a Rigorous Test of Statistical Theories. *J. Chem. Phys.* **2005**, *122*, 194312.

26 Yin, H. M.; Kable, S. H.; Zhang, X.; Bowman, J. M. Signatures of H2CO Photodissociation from Two Electronic States. *Science* **2006**, *311*, 1443–1446.

27 Valachovic, L. R.; Tuchler, M. F.; Dulligan, M.; Droz-Georget, T.; Zyrianov, M.; Kolessov, A.; Reisler, H.; Wittig, C. Photoinitiated H2CO Unimolecular Decomposition: Accessing H + HCO Products via S0 and T1 Pathways. *J. Chem. Phys.* **2000**, *112*, 2752–2761.

28 Seakins, P. W.; Leone, S. R. A Laser Flash Photolysis/Time-Resolved FTIR Emission Study of a New Channel in the Reaction of CH₃ + O: Production of CO(v). *J. Phys. Chem.* **1992**, *96*, 4478–4485.

29 Marcy, T. P.; Diaz, R. R.; Heard, D.; Leone, S. R.; Harding, L. B.; Klippenstein, S. J. Theoretical and Experimental Investigation of the Dynamics of the Production of CO from the CH₃ + O and CD₃ + O Reactions. *J. Phys. Chem. A* **2001**, *105*, 8361–8369.

30 Mohammad, F.; Morris, V. R.; Fink, W. H.; Jackson, W. M. On the Mechanism and Branching Ratio of the CN + O₂ → CO + NO Reaction Channel Using Transient IR Emission Spectroscopy. *J. Phys. Chem.* **1993**, *97*, 11590–11598.

31 Pomerantz, A. E.; Camden, J. P.; Chiou, A. S.; Ausfelder, F.; Chawla, N.; Hase, W. L.; Zare, R. N. Reaction Products with Internal Energy beyond the Kinematic Limit Result from Trajectories Far from the Minimum Energy Path: An Example from H + HBr → H₂ + Br. *J. Am. Chem. Soc.* **2005**, *127*, 16368–16369.

32 Lopez, J. G.; Vayner, G.; Lourderaj, U.; Addepalli, S. V.; Kato, S.; Dejong, W. A.; Windus, T. L.; Hase, W. L. A Direct Dynamics Trajectory Study of F⁻ + CH₃OOH Reactive Collisions Reveals a Major Non-IRC Reaction Path. *J. Am. Chem. Soc.* **2007**, *129*, 9976–9985.

33 Mann, D. J.; Hase, W. L. Ab Initio Direct Dynamics Study of Cyclopropyl Radical Ring-Opening. *J. Am. Chem. Soc.* **2002**, *124*, 3208–3209.

34 Nazar, M. A.; Polanyi, J. C.; Skrlac, W. J. Energy Distribution among Reaction Products. H + NOCl, H + ICl. *Chem. Phys. Lett.* **1974**, *29*, 473–479.

35 Townsend, D.; Minitti, M. P.; Suits, A. G. Direct Current Slice Imaging. *Rev. Sci. Instrum.* **2003**, *74*, 2530–2539.

36 Eppink, A. T. J. B.; Parker, D. H. Velocity Map Imaging of Ions and Electrons Using Electrostatic Lenses: Application in Photoelectron and Photofragment Ion Imaging of Molecular Oxygen. *Rev. Sci. Instrum.* **1997**, *68*, 3477–3484.

37 Chandler, D. W.; Houston, P. L. Two-Dimensional Imaging of State-Selected Photodissociation Products Detected by Multiphoton Ionization. *J. Chem. Phys.* **1987**, *87*, 1445–1447.

38 Li, W.; Chambreau, S. D.; Lahankar, S. A.; Suits, A. G. Megapixel Ion Imaging with Standard Video. *Rev. Sci. Instrum.* **2005**, *76*, 063106/063101–063106/063107.

39 Suits, A. G.; Chambreau, S. D.; Lahankar, S. A. State-Correlated DC Slice Imaging of Formaldehyde Photodissociation: Roaming Atoms and Multichannel Branching. *Int. Rev. Phys. Chem.* **2007**, *26*, 585–607.

40 Lahankar, S. A.; Goncharov, V.; Suits, F.; Farnum, J. D.; Bowman, J. M.; Suits, A. G. Further Aspects of the Roaming Mechanism in Formaldehyde Dissociation. *Chem. Phys.* **2008**, *347*, 288–299.

41 Harding, L. B.; Klippenstein, S. J.; Jasper, A. W. Ab Initio Methods for Reactive Potential Surfaces. *Phys. Chem. Chem. Phys.* **2007**, *31*, 4055–4070.

42 Houston, P. L.; Kable, S. H. Dissociation of Acetaldehyde at 308 nm: Another Example of the "Roaming" Mechanism? *Proc. Natl. Acad. Sci. U.S.A.* **2006**, *103*, 16079–16082.

43 Rubio-Lago, L.; Amaral, G. A.; Arregui, A.; Izquierdo, J. G.; Wang, F.; Zaouris, D.; Kitsopoulos, T. N.; Bañares, L. Slice Imaging of the Photodissociation of Acetaldehyde at 248 nm. Evidence of a Roaming Mechanism. *Phys. Chem. Chem. Phys.* **2007**, *9*, 6123–6127.

44 Shepler, B. C.; Braams, B. J.; Bowman, J. M. Quasiclassical Trajectory Calculations of Acetaldehyde Dissociation on a Global Potential Energy Surface Indicate Significant Non-transition State Dynamics. *J. Phys. Chem. A* **2007**, *111*, 8282–8285.